

Article

Curcumin Incorporated Poly(Butylene Adipate-co-Terephthalate) Film with Improved Water Vapor Barrier and Antioxidant Properties

Swarup Roy  and Jong-Whan Rhim *

Department of Food and Nutrition, BioNanocomposite Research Institute, Kyung Hee University, 26 Kyungheedaero, Dongdaemun-gu, Seoul 02447, Korea; swaruproy2013@gmail.com

* Correspondence: jwrhim@khu.ac.kr

Received: 16 August 2020; Accepted: 28 September 2020; Published: 30 September 2020



Abstract: Curcumin incorporated poly(butylene adipate-co-terephthalate) (PBAT) based film was fabricated. Curcumin has uniformly distributed in the PBAT matrix to form a bright yellow PBAT/curcumin film. The PBAT/curcumin film has slightly reduced tensile strength and flexibility than the neat PBAT film, while the thermal stability of the film has not changed significantly. The blending of curcumin significantly decreased the water vapor permeability of the PBAT film. Additionally, the PBAT/curcumin film showed potent antioxidant activity with some antimicrobial activity. The PBAT/curcumin films with improved water vapor barrier and additional functions can be used for active packaging applications.

Keywords: PBAT; curcumin; bioactive functional film; water vapor barrier property; antioxidant activity

1. Introduction

Petrochemical-based synthetic plastics gain popularity among all packaging materials due to their lightness, cost-effectiveness, user-friendliness, corrosion resistance, and structural properties [1]. Among the synthetic plastics commonly used in various packaging products are polypropylene, polystyrene, high and low-density polyethylene, polyethylene terephthalate, and polyvinyl chloride [2]. Plastics production worldwide has reached ~450 million tons each year, of which about 40% is used in the packaging industry [2]. The increase in plastics production is very alarming, and the growth rate of plastics production worldwide is expected to reach ~1800 million tons in 2050 [3]. Currently, there is an increasing demand for eco-friendly, biodegradable, and renewable plastics because too many non-biodegradable plastic packaging materials are generated, which can not only affect the environment and eco-systems but also cause serious plastic contamination [2,4,5]. Therefore, biodegradable and bio-based plastic packaging materials have gained significant attention for substituting non-biodegradable petroleum-based plastic polymers [6–8]. Biodegradable plastics are much more environmentally-friendly than petroleum-based plastics because they are easily decomposed by microorganisms in the environment, producing carbon dioxide and water [9,10]. Polyesters such as PBAT (poly(butylene adipate-co-terephthalate)), PLA (poly(lactide)), and PHA (poly(hydroxy alkanooates)) are of great interest due to their biodegradability and hydrolysis of ester bonds to non-toxic substances [11,12]. Among these polyesters, PBAT is considered one of the most likely biodegradable polymers for food packaging film applications [13–15]. PBAT is an aliphatic, aromatic polyester, mainly obtained from 1,4-butanediol, adipic acid, and terephthalic acid. PBAT is readily dissolved in chloroform, making it possible to prepare PBAT film using a simple solution casting technique. The aliphatic portion of PBAT provides good biodegradability, and the aromatic

portion provides good mechanical properties [16]. PBAT is also very flexible, which is useful for flexible packaging applications [17]. Despite the useful functional properties of PBAT, its use is sometimes limited due to its weak barrier properties [9,17]. Therefore, it is necessary to expand the properties of the PBAT film to replace the petroleum-based polymers currently used in the packaging area. A variety of functional or reinforcing fillers such as SiO₂, graphene oxide, MgO, AgNP, ZnONP, clay, curcumin, grape seed extract, etc. have been utilized to enhance the physical and functional properties of PBAT films [9,15,17–25]. In this sense, the use of natural bioactive compounds to improve PBAT film properties is an attractive field of research.

Curcumin, a natural bioactive compound, is interesting because it is non-toxic and shows numerous benefits and applications that are already very well known [26–28]. Curcumin is a hydrophobic phenolic substance derived from *Curcumin longa*, also known as turmeric, and has long been used as a spice in food and medicine to treat various diseases [28]. Although curcumin has high clinical applicability, its low water solubility, absorbability, and metabolism have limited its direct use in biomedicine [29]. Curcumin has been used to produce functional films mixed with various polymers such as PLA, PBAT, LDPE, cellulose, pectin, carrageenan, gelatin, etc. for biomedical and food packaging applications [21,30–39]. Recently, De Compos et al. reported the preparation of curcumin-reinforced PBAT and thermoplastic cassava starch-based extruded composite films [21]. In addition, PBAT-based electrospun nanofiber has been developed by reinforcing curcumin and 5-fluorouracil [39]. As far as we know, there are no reports of concentration-dependent curcumin effects on the film properties of PBAT-based films using the solution casting method for active packaging applications. The solution casting method is simple and useful for testing the effectiveness of fillers and determining laboratory-scale processing conditions. The information obtained can be used for large-scale production using the extrusion method. Curcumin is a useful bioactive natural functional compound used very recently to make functional films compounded with various bioplastics. PBAT is the right candidate for making functional packaging film compounded with curcumin. Since both PBAT and curcumin are soluble in the same solvent (chloroform), the solution casting method is the right choice for preparing the PBAT/curcumin blending film. The addition of curcumin to PBAT-based film is likely to improve the physical and functional properties of the film.

The main objective of the present work was to prepare a functional PBAT-based film by mixing with curcumin. The bioactive film was characterized using various analytical methods. Additionally, the effect of various concentrations of curcumin on different physical (surface color, optical, mechanical, and water vapor barrier properties) and functional properties (antioxidant and antimicrobial) and the release profile of curcumin from the PBAT-based films were investigated.

2. Materials and Methods

2.1. Materials

PBAT (EnPol PBG7070; m.p. 125 °C, the specific gravity of 1.20–1.25) was acquired from S-EnPol Co. Ltd., (Wonju, Korea). Curcumin, DPPH, ABTS, and potassium persulfate were purchased from Sigma-Aldrich, (St. Louis, MO, USA). Chloroform and ascorbic acid were procured from Daejung Chemicals and Metals Co., Ltd., (Siheung, Korea). TSB, BHI media, and agar powder were purchased from Duksan Pure Chemicals Co., Ltd., (Ansan, Korea). *Escherichia coli* O157: H7 ATCC 43895 and *Listeria monocytogenes* ATCC 15313 were acquired from the Korean Collection for Type Culture (KCTC, Seoul, Korea).

2.2. Fabrication of PBAT/Curcumin Films

The PBAT/curcumin films were fabricated using a solution casting method [19]. Various amounts of curcumin (0.125, 0.25, 0.5, and 1.0 wt% of PBAT) were dissolved in 100 mL of chloroform with stirring for 1 h and added 4 g of PBAT to the curcumin solution and mixed with vigorous stirring for 24 h. The film solution was then cast on a leveled Teflon film-coated glass plate and evaporated the

solvent in a fume hood for 48 h. Then the dried film was peeled off the plate and conditioned for at least 48 h in a humidity chamber controlled at 25 °C and 50% RH. For comparison, a neat PBAT film without curcumin was also produced according to the prescribed method. All films were made in triplicate and used as experimental replication units. The prepared films were designated PBAT/cur^{0.125}, PBAT/Cur^{0.25}, PBAT/Cur^{0.5}, and PBAT/Cur^{1.0}, respectively, according to the curcumin content.

2.3. Characterization and Properties of PBAT/Curcumin Film

2.3.1. Surface Morphology

The microstructure (surface and cross-section) of the film was observed using a field emission scanning electron microscope (FE-SEM, SU-8000, Hitachi Co., Ltd., Matsuda, Japan).

2.3.2. Thermal Analysis

The thermal stability of the film and curcumin was tested using a thermogravimetric analyzer (Hi-Res TGA 2950, TA Instrument, New Castle, DE, USA) following the method of Roy et al. [40]. The temperature of the maximum disintegration rate was determined from a derivative form of the TGA (DTG) curve, and the weight loss (%) was calculated from the TGA curve [40].

The melt-crystallization of the film samples was evaluated using a differential scanning calorimeter (DSCQ100, TA Instruments, New Castle, DE, USA), and the transition temperature was calculated from the DSC thermogram following the method of Sousa et al. [41].

2.3.3. Surface Color and Optical Properties

The surface color of the film samples was assessed using a Chroma meter (Konica Minolta, CR-400, Tokyo, Japan). The Hunter color (L , a , b) of the film sample was obtained, and the total color difference (ΔE) was computed using Equation (1).

$$\Delta E = [(\Delta L)^2 + (\Delta a)^2 + (\Delta b)^2]^{0.5} \quad (1)$$

where ΔL , Δa , and Δb is the difference of each color values between the standard color plate and film sample, respectively. The yellowness index (YI) of the film was determined using Equation (2).

$$YI = (142.86 \times b)/L \quad (2)$$

The optical properties of the films were evaluated using a UV-vis spectrophotometer (Mecasys Optizen POP Series UV/Vis, Seoul, Korea). The light absorbance of the film was taken in the wavelength range of 200 nm–800 nm. UV-barrier and transparency properties of the film samples were assessed by measuring the light transmittance at 280 nm (T_{280}) and 660 nm (T_{660}), respectively [34].

2.3.4. Mechanical Properties

A digital micrometer (QuantuMike IP 65, Mitutoyo, Japan) with an accuracy of 1 μm was used to measure the thickness of the film samples [40].

The mechanical properties were measured using an Instron Universal Testing Machine (Model 5565, Instron Engineering Corporation, Canton, MA, USA) following the standard ASTM method D 882-88. The machine was operated with an initial grip separation of 50 mm and a crosshead speed of 50 mm/min using a 500 N load cell [27].

2.3.5. Water Vapor Permeability (WVP) and Water Contact Angle (WCA)

The water vapor permeability (WVP) of the film sample was measured at 25 °C under 50% RH conditions [27]. First, the water vapor transmission rate (WVTR, $\text{g}/\text{m}^2 \text{ s}$) was determined according to the ASTM E96-95 method. For this, 18 mL of distilled water was added to the WVP cup (6.8 cm

diameter and 2.5 cm depth) made of poly(methylmethacrylate), fixed the film sample on the cup, and sealed tightly. The assembled WVP cup was put in a humidity chamber (25 °C and 50% RH), and measured the weight change periodically. The WVTR of the film was calculated from the slope of the weight change of the WVP cup vs. time curve, and the WVP (g m/m² Pa.s) of the film was computed using Equation (3).

$$\text{WVP} = (\text{WVTR} \times L) / \Delta p \quad (3)$$

where L was the mean film thickness (m), and Δp was the partial water vapor pressure difference across the two sides of the film [42].

The water contact angle of the film was determined using the water contact angle (WCA) analyzer (Phoneix 150, Surface Electro Optics Co., Ltd., Kunpo, Korea). For this, the film sample was positioned on the WCA analyzer, and 10 μ L of water drop was added to the film and measured the WCA immediately [43].

2.4. Curcumin Releasing Test

The quantity of curcumin released from the PBAT/curcumin film into the water was determined following Roy and Rhim [27]. For this, the test film (PBAT/Cur^{0.25} and PBAT/Cur^{1.0}) samples (2.5 cm \times 2.5 cm) were transferred in 20 mL of distilled water and incubated at 37 °C. A 2 mL solution sample was taken at predetermined intervals and measured the absorbance of the sample at 420 nm.

2.5. Antibacterial Activity

The antibacterial activity of the film was evaluated against foodborne pathogenic bacteria, *E. coli* and *L. monocytogenes* [34]. The test bacteria were first aseptically inoculated into TSB and BHI broth, respectively, and incubated at 37 °C for 24 h. After properly diluting the culture, 200 μ L of the diluted inoculum (10⁸–10⁹ CFU/mL) was aseptically transferred to 50 mL of TSB and BHI broth, respectively, together with 200 mg of the film samples to reach the initial concentration of bacteria around 10⁶ CFU/mL, and incubated at 37 °C for 12 h with shaking at 100 rpm. Samples were taken at predetermined intervals, and the number of viable cells was measured by diluting and plating samples on agar plates.

2.6. Antioxidant Activity

The antioxidant activity of curcumin and PBAT/curcumin film samples was evaluated using DPPH[•] and ABTS^{•+} free radical scavenging activities [33,44]. For the DPPH assay of the PBAT/curcumin film, a predetermined amount of the films were added to 10 mL DPPH solution and measured the absorbance at 517 nm after 24 h. For the ABTS analysis, a predetermined amount of the test films were mixed with 10 mL of ABTS assay solution and measured the absorbance at 734 nm after 24 h. The antioxidative activity of the films was calculated using Equation (4):

$$\text{Free radical scavenging activity (\%)} = \frac{A_0 - A_T}{A_0} \times 100 \quad (4)$$

where A_0 and A_T was the absorbance of DPPH or ABTS of the control and test film, respectively. All the test was performed in triplicate, and the average value was reported.

2.7. Statistical Analysis

Film properties were measured in triplicates of separately prepared films, and the results were presented as mean \pm SD (standard deviation). ANOVA test was performed, and the significant difference ($p < 0.05$) among treatment groups was separated by Duncan's multiple range test using the SPSS computer program (SPSS Inc., Chicago, IL, USA).

3. Results and Discussion

3.1. Morphology

All films were smooth and flexible without any defects. The surface microstructure of the neat PBAT and PBAT/curcumin films is shown in Figure 1a–c. It showed the smooth-surfaced films, in which curcumin was evenly dispersed in the PBAT matrix. At a small amount of curcumin, it formed a compatible film with the PBAT without creating an aggregation of the particle. Even at high curcumin (1 wt%), the film surface was smooth without any cavity between curcumin and PBAT polymer. The cross-sectional FESEM images (Figure 1d–i) also showed well-dispersed curcumin in the PBAT matrix when the curcumin content was low, while curcumin was aggregated when a higher content was added. The morphology of the films designated that the curcumin was blended compatibly with the PBAT matrix. Similarly, curcumin was reported to be well dispersed in LDPE and cellulose-based films [31,45]. The FESEM image of curcumin (Figure 1j) showed that curcumin has an asymmetrical form that complies with previously published reports [34].

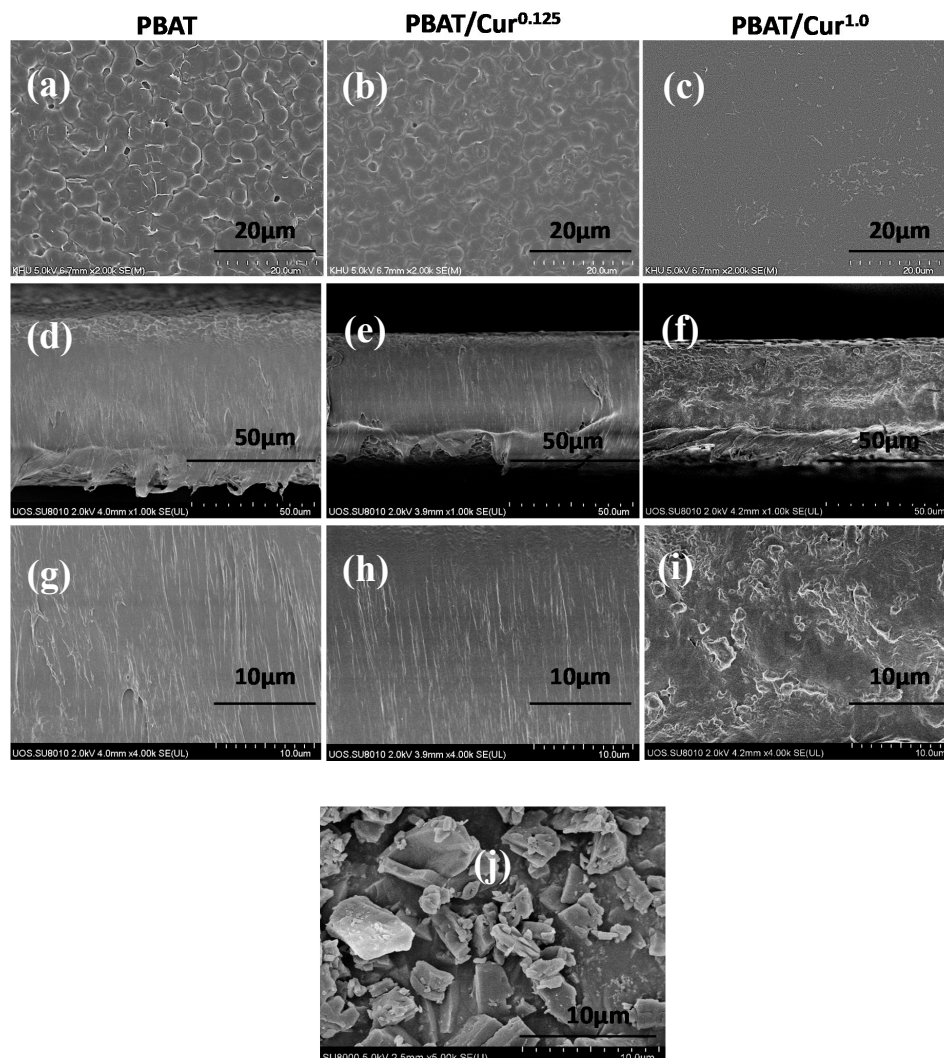


Figure 1. FE-SEM pictures of surface (a–c) and cross-section (d–h) of the neat poly(butylene adipate-co-terephthalate) (PBAT) and PBAT/curcumin films (d–f: low and g–i: high magnification) and FE-SEM image of curcumin powder (j).

3.2. Thermostability

Figure 2 shows the TGA and DTG thermograms of the neat PBAT, PBAT/curcumin films with low (0.125 wt%) and high content (1.0 wt%) of curcumin and curcumin powder. All films exhibited one-step thermal decomposition at 350 °C–430 °C with maximal degradation at 398 °C. Similar thermal degradation patterns were observed in PBAT/silver nanoparticle films [19]. The remaining char content of the PBAT film was ~8% and enhanced a little after mixing with curcumin. In curcumin powder, the thermal decomposition pattern was different from the PBAT film, although the maximum degradation temperature was in a similar temperature range. The analysis data of the thermal degradation of PBAT/curcumin films and curcumin powder were shown in Table 1. The TGA test results showed that the thermal stability PBAT was not affected by the blending of curcumin. Current results were also consistent with previously published reports [34].

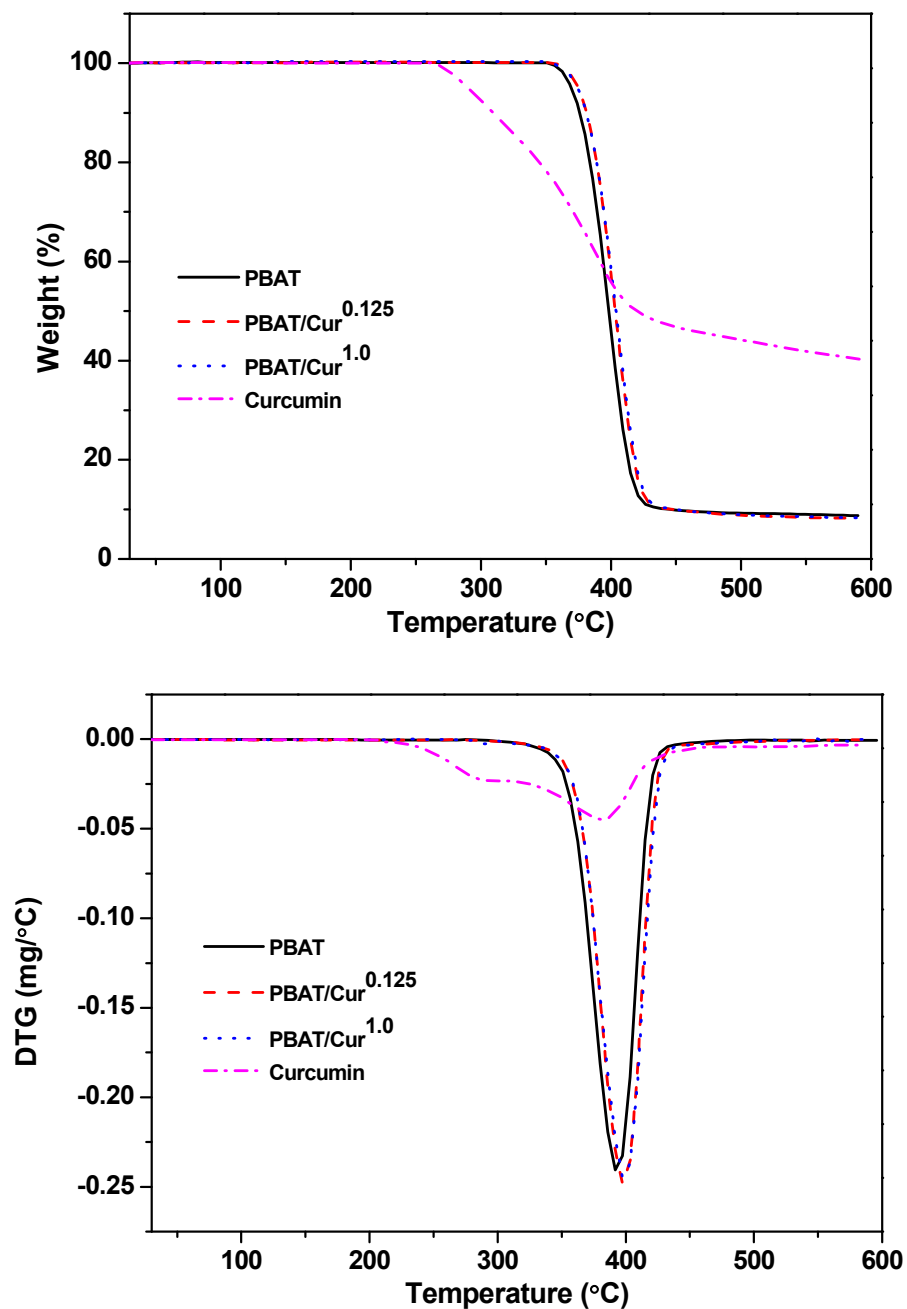
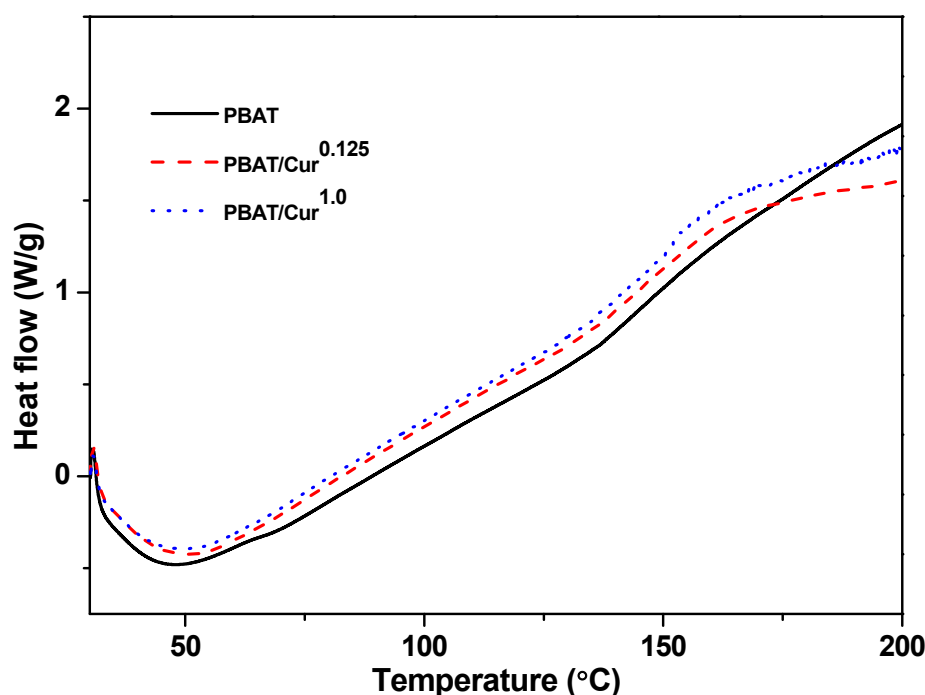


Figure 2. TGA and DTG thermograms of the neat PBAT and PBAT/curcumin films and curcumin powder.

Table 1. TGA results of the films and curcumin powder.

Sample	$T_{0.5}$ (50%) (°C)	Char Content (%)	T_{max} (°C)
PBAT	402.6 ± 4.0	7.7 ± 0.9	395.8 ± 3.6
PBAT/Cur ^{0.125}	404.2 ± 1.4	7.8 ± 0.4	397.7 ± 0.2
PBAT/Cur ^{1.0}	404.4 ± 0.7	7.8 ± 0.4	397.7 ± 0.2
Curcumin	424.7 ± 6.7	41.0 ± 1.2	381.0 ± 1.3

The DSC thermograms of the films are presented in Figure 3. Glass transition was observed around 50 °C in both PBAT and PBAT/curcumin blend films. The similar glass transition temperatures of the neat PBAT and PBAT/curcumin films showed that the blending of curcumin did not pointedly modify the structure of PBAT, indicating curcumin was well-blended with the PBAT polymer matrix.

**Figure 3.** DSC thermogram neat PBAT and PBAT/curcumin film.

3.3. Surface Color and Optical Properties

The visual appearance of the PBAT and PBAT/curcumin films are displayed in Figure 4. The neat PBAT film was translucent without any hue but became yellow by the addition of curcumin and became more yellow with increasing curcumin content. The surface color values of the PBAT/curcumin films are presented in Table 2. The L -value (brightness) of the PBAT film improved somewhat with the blending of 0.125 wt% curcumin, then decreased linearly with increasing curcumin content. On the other hand, the a -value (greenness) decreased significantly with the addition of 0.125 wt% of curcumin and enhanced with increasing curcumin content. However, the b -value (yellowness) increased profoundly by the blending of curcumin, indicating a hyperbolic increase pattern according to the curcumin content. Accordingly, the ΔE of the films was also enhanced considerably by the blending of curcumin, and it also increased the hyperbolic manner with the curcumin concentration. The YI of the PBAT-based film was pointedly enhanced by the blending of curcumin, which was reliant on the curcumin content. Likewise, it was stated that the surface color of the gelatin-based film also transformed greatly depending on the amount of curcumin added [32,33].

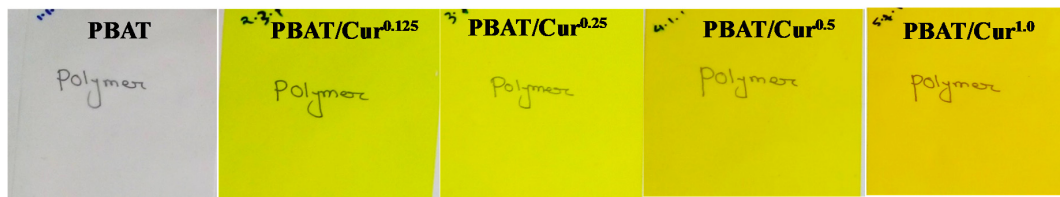


Figure 4. The visual appearance of the neat PBAT and PBAT/curcumin films.

Table 2. Apparent color and light transmittance of the neat PBAT and PBAT/curcumin films.

Films	<i>L</i>	<i>a</i>	<i>b</i>	ΔE	<i>YI</i>	<i>T</i> ₂₈₀ (%)	<i>T</i> ₆₆₀ (%)
PBAT	92.3 ± 0.1 ^b	−0.29 ± 0.0 ^c	4.4 ± 0.1 ^a	0.3 ± 0.1 ^a	6.9 ± 0.2 ^a	0.03 ± 0.01 ^a	5.0 ± 0.8 ^a
PBAT/Cur ^{0.125}	93.4 ± 0.4 ^d	−25.6 ± 0.1 ^a	74.5 ± 2.4 ^b	73.6 ± 2.3 ^b	113.9 ± 4.0 ^b	0.03 ± 0.01 ^a	5.7 ± 1.4 ^a
PBAT/Cur ^{0.25}	93.2 ± 0.1 ^d	−23.4 ± 0.1 ^b	81.9 ± 2.6 ^c	80.6 ± 2.5 ^c	125.5 ± 4.0 ^c	0.04 ± 0.01 ^{ab}	5.9 ± 1.7 ^a
PBAT/Cur ^{0.5}	92.7 ± 0.1 ^c	−21.9 ± 0.9 ^c	89.9 ± 0.7 ^d	87.9 ± 0.5 ^d	138.6 ± 1.2 ^d	0.06 ± 0.01 ^c	6.0 ± 1.1 ^a
PBAT/Cur ^{1.0}	89.6 ± 0.1 ^a	−12.5 ± 0.1 ^d	92.5 ± 0.7 ^d	88.7 ± 0.7 ^d	147.5 ± 1.3 ^e	0.04 ± 0.01 ^{ab}	7.1 ± 1.0 ^a

The values are presented as a mean ± standard deviation. Different letters (such as a, b, etc.) within the same column indicate significant differences ($p < 0.05$) by Duncan's multiple range test.

The UV-visible light absorption profile of films are shown in Figure 5. The PBAT film had no visible light absorption peak, but the PBAT/curcumin film exhibited a peak at ~420 nm owing to the presence of curcumin. The peak at low curcumin content (<0.25 wt%) was sharp, but it became broadened at high curcumin content (>0.5 wt%). It was also observed that the light absorption of visible light (>500 nm) of the PBAT/curcumin film were lower or comparable to that of the PBAT film, suggesting that the PBAT/curcumin film is more transparent than the neat PBAT film. Similar light absorption phenomena have been observed in the PBAT/silver nanoparticles films [19]. The PBAT film prevented UV light transmittance nearly completely, which showed the T_{280} of 0.03% (Table 2). It is evident that the PBAT film has high UV-barrier property, which is mainly due to the many UV-light absorbing functional groups in the PBAT [19]. The PBAT film was translucent, having a T_{660} of 5.0%. The transparency of the PBAT film improved a little, which was also evidenced in the light absorption test (Figure 5), but the change was not statistically significant ($p > 0.05$).

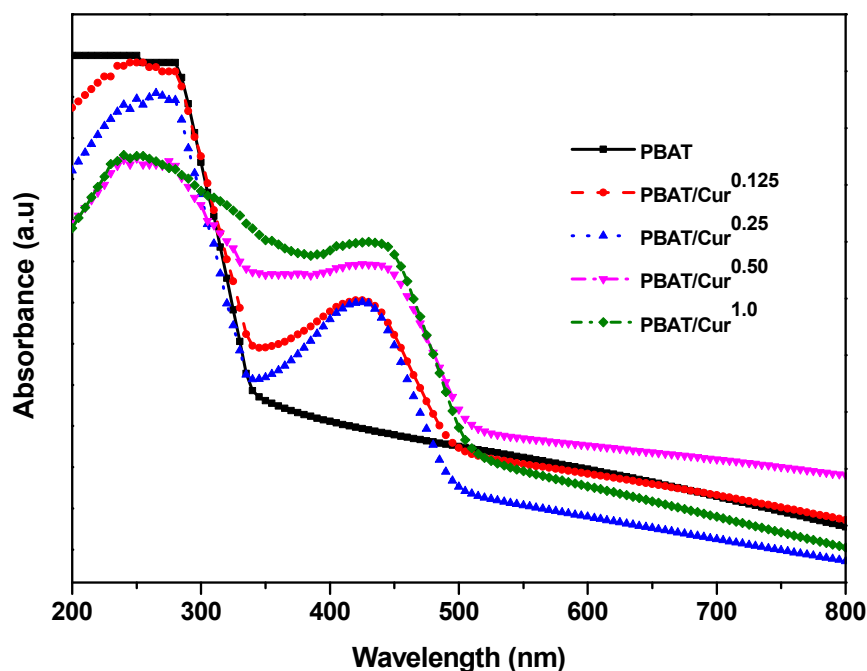


Figure 5. UV-vis light absorption spectra of the neat PBAT and PBAT/curcumin film.

3.4. Mechanical Properties

The thickness and mechanical behaviors of the films are presented in Table 3. The thickness of the PBAT film increased slightly by the addition of curcumin of less than 0.5 wt%, but it pointedly enhanced ($p < 0.05$) when added a high amount of curcumin (1 wt%). The increased thickness of the film was possibly owing to the enhanced solid content by the addition of curcumin. The mechanical properties of the PBAT film were also influenced by the incorporation of curcumin. The TS of the neat PBAT film was 8.0 ± 0.5 MPa, indicating it is a flexible film with low strength [19]. The TS of the PBAT film decreased a little by the blending of curcumin, which reduced to 6.0 ± 1.1 MPa when 1.0 wt% of curcumin was added. The EB of the neat PBAT film was $23.8\% \pm 2.3\%$, representing that the PBAT film is elastic; however, the elasticity of PBAT film reduced a little by the blending of curcumin. The EM (rigidity of the film) of the PBAT film was not changed when a low level of curcumin (0.125 wt%) was added but decreased slightly when more than 0.25 wt% of curcumin was blended. Previously, it was reported that the blending of curcumin did not influence the mechanical behaviors of PBAT films, which might be owing to the compatible and even distribution of curcumin in the polymer matrix, also the appropriate interfacial interactions among them. The present observation was also in compliance with the previously published report [34,45]. Additionally, the blending of curcumin did not change the mechanical properties significantly in the gelatin-based films [32,33]. On the other hand, adding curcumin to the PLA-based film [46] and adding grapefruit seed extract (GSE) to the PLA/PBAT blend film [20] improved the mechanical behaviors of the film.

Table 3. Mechanical properties, water vapor permeability (WVP), and water contact angle (WCA) of the neat PBAT and PBAT/curcumin films.

Films	Thickness (μm)	TS (MPa)	EB (%)	EM (MPa)	WVP ($\times 10^{-11}$ g·m/m ² ·Pa·s)	WCA (deg.)
PBAT	54.6 ± 4.1^a	8.0 ± 0.5^b	23.8 ± 2.3^c	88.1 ± 2.8^c	7.1 ± 0.7^c	55.9 ± 2.4^a
PBAT/Cur ^{0.125}	55.6 ± 1.4^a	6.4 ± 0.1^a	17.4 ± 0.8^a	88.9 ± 2.4^c	6.9 ± 0.5^{ab}	57.7 ± 3.2^{ab}
PBAT/Cur ^{0.25}	58.0 ± 1.8^a	6.8 ± 0.3^a	19.9 ± 1.5^{ab}	81.0 ± 6.1^{ab}	6.3 ± 0.5^{ab}	59.5 ± 3.1^b
PBAT/Cur ^{0.5}	58.9 ± 1.8^a	6.7 ± 0.4^a	22.7 ± 2.3^c	77.2 ± 2.3^a	5.9 ± 0.6^a	63.2 ± 2.0^c
PBAT/Cur ^{1.0}	64.7 ± 2.4^b	6.0 ± 1.1^a	18.8 ± 0.4^a	82.6 ± 4.0^{ab}	5.8 ± 0.4^a	63.3 ± 3.6^c

The values are presented as a mean \pm standard deviation. Different letters (such as a, b, etc.) within the same column indicate significant differences ($p < 0.05$) by Duncan's multiple range test.

3.5. WVP and WCA

The WVP of the films are presented in Table 3. The WVP of the neat PBAT film was $7.1 \pm 0.7 \times 10^{-11}$ g·m/m²·Pa·s, which was reduced significantly ($p < 0.05$) by the addition of curcumin. The WVP of the PBAT film decreased to $5.8 \pm 0.4 \times 10^{-11}$ g·m/m²·Pa·s when 1.0 wt% of curcumin was added. The decreased WVP of the film may be due to the reduced hydrophilicity of the PBAT film through the introduction of hydrophobic curcumin in the PBAT polymer matrix, which hindered the water vapor diffusion and reduced the WVP of the film. The hydrophobic curcumin dispersed in the polymer matrix may reduce water vapor dissolution and diffusion to reduce the WVP. Besides, the rise in the vapor barrier properties of PBAT films with the incorporation of curcumin may be due to an increase in the density of the film or a decrease in free volume after mixing with curcumin (Figure 1). It has been stated that the blending of curcumin to PLA-based film reduced the WVP, whereas the addition of GSE to PLA/PBAT composite film reduced the water vapor barrier properties [20,47]. On the contrary, the addition of impermeable nanoparticles such as silver nanoparticles and graphene oxide was supposed to form a tortuous path of water vapor diffusion in the PBAT film to reduce the WVP [17,19].

The hydrophobicity of the neat PBAT and PBAT/curcumin films was assessed by determining the WCA (Table 3). The WCA of the neat PBAT film was $55.9^\circ \pm 2.4^\circ$, suggesting that the PBAT film has a water-absorbing surface. The WCA of PBAT film significantly increased ($p > 0.05$) by the blending of curcumin, depending on the content of curcumin. The increase in the WCA of PBAT-based films most

probably because of the hydrophobic nature of curcumin [33]. The addition of curcumin to PLA-based film also pointedly enhanced the surface hydrophobicity of the film [47]. Additionally, the improved surface water-resistant activity by incorporating curcumin was described in previous reports [31,34,47].

3.6. Release of Curcumin

The release of curcumin from the PBAT/curcumin film is shown in Figure 6. The rate of release of curcumin was dependent on the concentration of curcumin. However, for a high curcumin content (1.0 wt%), the amount of curcumin released increased linearly with immersion time. The release rate of curcumin depends on the curcumin content and polymer matrix. A more quick release of curcumin has been observed from carbohydrate-based films and guar gum-based films [27,48]. The slow-release of curcumin from the PBAT-based films was due to the low swelling of the polymer matrix in water and low water solubility of curcumin. The degree of release of the bioactive molecule from the film depends on several aspects like the kind of the polymer matrix, swelling of polymers, and interaction between the polymer and the filler as well as the rate of dissolution and diffusion of the compound in the film matrix and the solubility of the compound in the immersion solution [49].

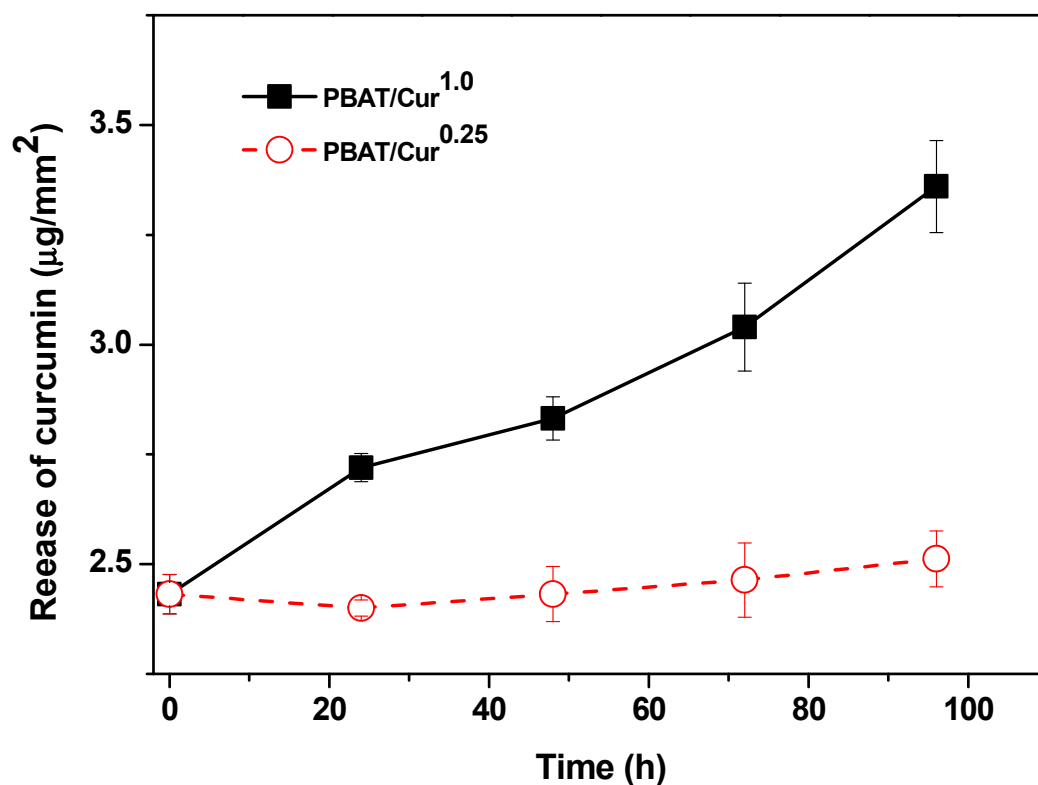


Figure 6. The releasing pattern of curcumin from the PBAT/curcumin film.

3.7. Antimicrobial Activity

As expected, the neat PBAT film showed no antibacterial activity, but the curcumin-added films showed a slight antibacterial activity against both *E. coli* and *L. monocytogenes* (Figure 7). The PBAT/curcumin film did not destroy the bacteria but showed an apparent antibacterial activity that reduces the growth rate of the test bacteria. Depending on the content of curcumin, the film showed a 1–2 log (CFU) lower growth of test bacteria compared to the control groups at 12 h of the test period. Since the neat PBAT film has no antibacterial activity, it can be concluded that the antibacterial function of PBAT/curcumin film is attributed to curcumin [50]. Similar antibacterial activity has been reported for the case of cellulose/curcumin film [34,45]. The small antibacterial activity of the PBAT/curcumin film can be ascribed to the low curcumin content, the slow release of curcumin, and the specificity of the

test microbial strain for curcumin. There are reports of high antibacterial activity of curcumin against various fungal and bacterial strains [50]. Conversely, it has been reported that the gelatin/curcumin film does not have a significant antibacterial effect against *S. enteritidis*, *E. coli*, *B. cereus*, and *S. aureus* [32], which may be due to the low curcumin content in the gelatin-based film. Curcumin's antibacterial activity relies on the interruption of FtsZ role, an essential protein required for bacterial cellular division [51]. The possible antimicrobial activity of curcumin is thought to be because curcumin binds to the FtsZ protein, stopping the joining of the FtsZ protofilament, disrupting the construction of the Z-ring, and impeding cell movement and bacterial development [51]. Curcumin is recognized to increase the GTPase action of the FtsZ protein [52]. It was also believed that the antimicrobial action of curcumin was related with membrane destruction over the binding of the curcumin and peptidoglycan layers of the bacteria [53].

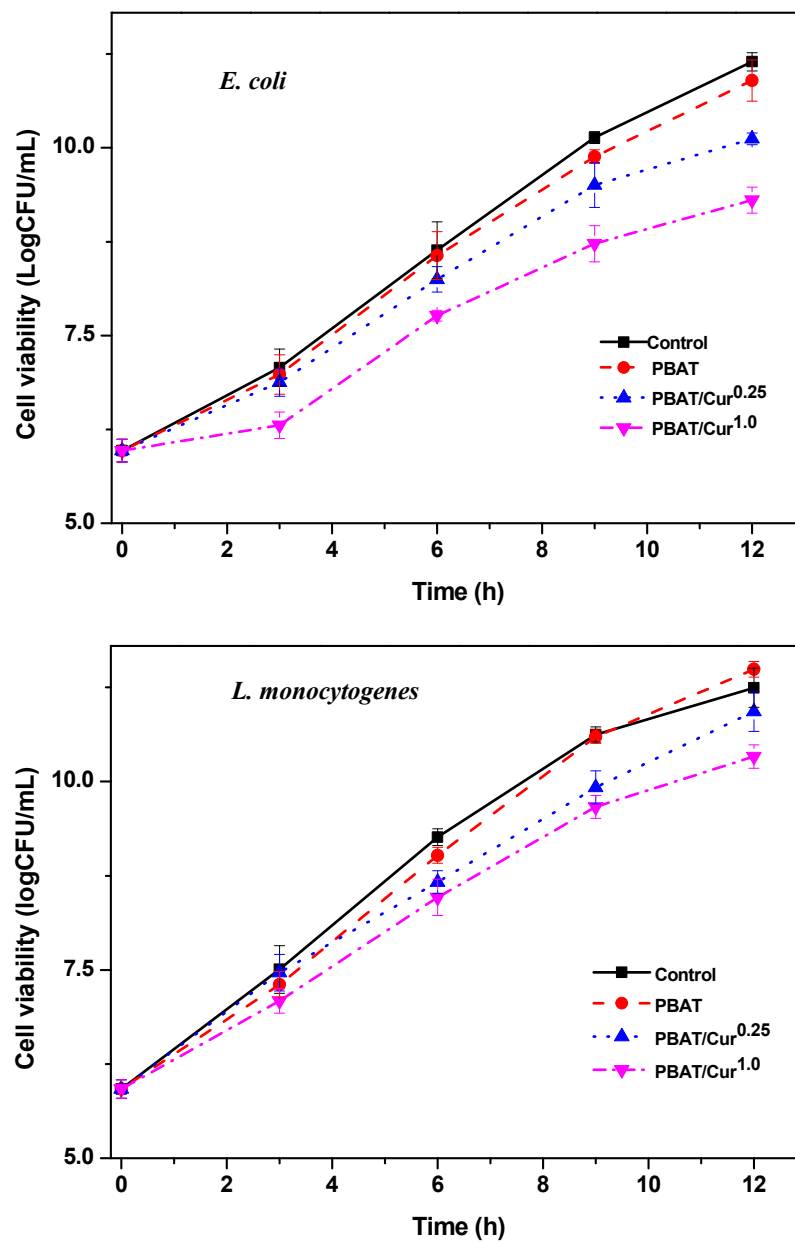


Figure 7. Antibacterial activity of the neat PBAT and PBAT/curcumin films against *E. coli* and *L. monocytogenes*.

3.8. Antioxidant Activity

Because curcumin is a well-known antioxidant [54], the PBAT/curcumin films are also expected to show antioxidant activity. The antioxidant activity of PBAT/curcumin films was evaluated, and the results are shown in Figure 8. As expected, the PBAT/curcumin film showed potent antioxidant activity, and the activity was dependent on the curcumin content. The DPPH and ABTS scavenging activities of the neat PBAT film were 2.6% and 3.8%, respectively, which increased to 93.5% and 88.7%, respectively, after forming the film with 1.0 wt% of curcumin. The high antioxidant activity of curcumin comes from the H-atomic donation function of the curcumin phenol group [54]. The addition of curcumin also provided a strong antioxidant activity for various edible films [32–34]. The PBAT/curcumin films can be used as antioxidant packaging for foods that are prone to oxidative degradation.

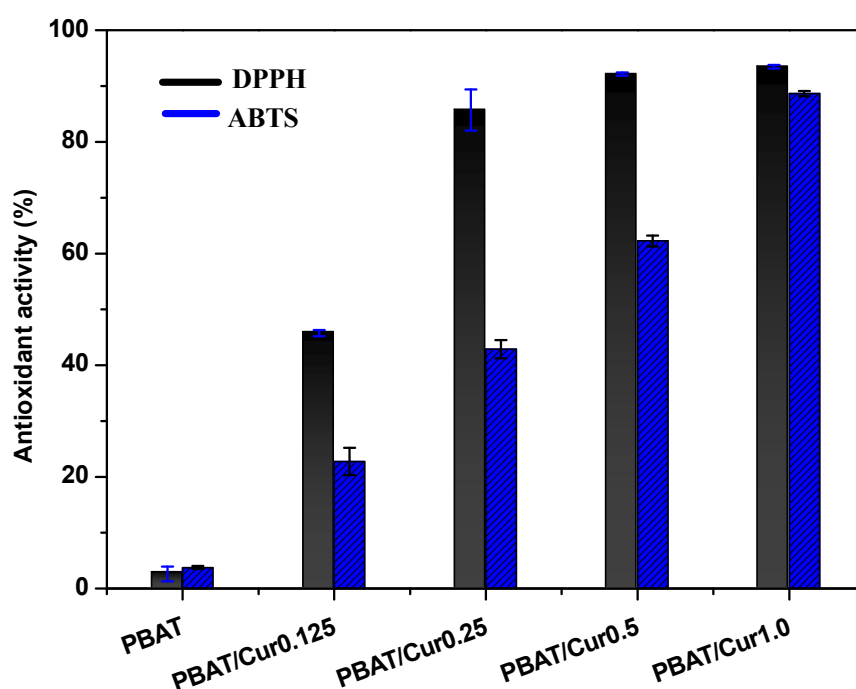


Figure 8. Antioxidant activity of the neat PBAT and PBAT/curcumin films determined by DPPH and ABTS assay.

4. Conclusions

The PBAT/curcumin films were fabricated using a solution casting technique. The addition of curcumin affected the surface color, mechanical, water vapor barrier, and antioxidant properties of the PBAT films. The curcumin was uniformly dispersed in the PBAT film and showed a typical light absorption peak at 420 nm. The mechanical properties of the film were slightly decreased after the incorporation of curcumin, whereas the thermal stability of the films was not influenced. The water vapor barrier property of the PBAT/curcumin film was significantly enhanced. The PBAT/curcumin films exhibited high antioxidant activity and some antimicrobial activity against foodborne pathogenic bacteria. The PBAT/curcumin film with increased water vapor barrier and antioxidant activity can be used for food packaging applications to extend the shelflife of food.

Author Contributions: Conceptualization, S.R. and J.-W.R.; methodology, S.R.; software, S.R.; validation, S.R. and J.-W.R.; formal analysis, S.R.; investigation, S.R.; resources, J.-W.R.; data curation, S.R.; writing—original draft preparation, S.R.; writing—review and editing, J.-W.R.; visualization, J.-W.R.; supervision, J.-W.R.; project administration, J.-W.R.; funding acquisition, J.-W.R. All authors have read and agree to the published version of the manuscript.

Funding: This research was funded by the National Research Foundation of Korea (NRF) grant funded by the Korea government (MSIT) (No. 2019R1A2C2084221).

Acknowledgments: This work was supported by the National Research Foundation of Korea (NRF) grant funded by the Korea government (MSIT) (No. 2019R1A2C2084221).

Conflicts of Interest: The authors declare there is no conflict of interest.

References

1. Jambeck, J.R.; Geyer, R.; Wilcox, C.; Siegler, T.R.; Perryman, M.; Andrady, A.; Narayan, R.; Law, K.L. Marine pollution. Plastic waste inputs from land into the ocean. *Science* **2015**, *347*, 768–771. [[CrossRef](#)]
2. Geyer, R.; Jambeck, J.R.; Law, K.L. Production, use, and fate of all plastics ever made. *Sci. Adv.* **2017**, *3*, e1700782. [[CrossRef](#)]
3. Ryan, P.G. A brief history of marine litter research. In *Marine Anthropogenic Litter*; Springer International Publishing: New York, NY, USA, 2015; pp. 1–25. ISBN 9783319165103.
4. Ebnesajjad, S. *Handbook of Biopolymers and Biodegradable Plastics: Properties, Processing and Applications*; William Andrew: Waltham, MA, USA, 2012; pp. 1–472.
5. Li, W.C.; Tse, H.F.; Fok, L. Plastic waste in the marine environment: A review of sources, occurrence and effects. *Sci. Total Environ.* **2016**, *566–567*, 333–349. [[CrossRef](#)]
6. Halonen, N.; Pálvölgyi, P.S.; Bassani, A.; Fiorentini, C.; Nair, R.; Spigno, G.; Kordas, K. Bio-Based Smart Materials for Food Packaging and Sensors—A Review. *Front. Mater.* **2020**, *7*, 82. [[CrossRef](#)]
7. Jeya, J.; Chandrasekaran, M.; Venkatesan, S.P.; Sriram, V.; Britto, J.G.; Mageshwaran, G.; Durairaj, R.B. Scaling up difficulties and commercial aspects of edible films for food packaging: A review. *Trends Food Sci. Technol.* **2020**, *100*, 210–222. [[CrossRef](#)]
8. Roy, S.; Rhim, J.-W. Anthocyanin food colorant and its application in pH-responsive color change indicator films. *Crit. Rev. Food Sci. Nutr.* **2020**, *1–29*. [[CrossRef](#)] [[PubMed](#)]
9. Falcão, G.A.M.; Vitorino, M.B.C.; Almeida, T.G.; Bardi, M.A.G.; Carvalho, L.H.; Canedo, E.L. PBAT/organoclay composite films: Preparation and properties. *Polym. Bull.* **2017**, *74*, 4423–4436. [[CrossRef](#)]
10. Youssef, A.M.; El-Sayed, S.M. Bionanocomposites materials for food packaging applications: Concepts and future outlook. *Carbohydr. Polym.* **2018**, *193*, 19–27. [[CrossRef](#)]
11. Miller, S.A. Sustainable polymers: Opportunities for the next decade. *ACS Macro Lett.* **2013**, *2*, 550–554. [[CrossRef](#)]
12. Díez-Pascual, A.M.; Díez-Vicente, A.L. ZnO-reinforced poly(3-hydroxybutyrate-co-3-hydroxyvalerate) bionanocomposites with antimicrobial function for food packaging. *ACS Appl. Mater. Interfaces* **2014**, *6*, 9822–9834. [[CrossRef](#)]
13. Mondal, D.; Bhowmick, B.; Maity, D.; Mollick, M.M.R.; Rana, D.; Rangarajan, V.; Sen, R.; Chattopadhyay, D. Investigation on sodium benzoate release from poly(butylene adipate-co-terephthalate)/organoclay/sodium benzoate based nanocomposite film and their antimicrobial activity. *J. Food Sci.* **2015**, *80*, 602–609. [[CrossRef](#)] [[PubMed](#)]
14. Dammak, M.; Fourati, Y.; Tarrés, Q.; Delgado-Aguilar, M.; Mutjé, P.; Boufi, S. Blends of PBAT with plasticized starch for packaging applications: Mechanical properties, rheological behaviour and biodegradability. *Ind. Crop. Prod.* **2020**, *144*, 112061. [[CrossRef](#)]
15. Zhang, J.; Cao, C.; Zheng, S.; Li, W.; Li, B.; Xie, X. Poly (butylene adipate-co-terephthalate)/magnesium oxide/silver ternary composite biofilms for food packaging application. *Food Packag. Shelf Life* **2020**, *24*, 100487. [[CrossRef](#)]
16. Bastarrachea, L.; Dhawan, S.; Sablani, S.S.; Mah, J.-H.; Kang, D.-H.; Zhang, J.; Tang, J. Biodegradable poly(butylene adipate-co-terephthalate) films incorporated with nisin: Characterization and effectiveness against *Listeria innocua*. *J. Food Sci.* **2010**, *75*, 215–224. [[CrossRef](#)] [[PubMed](#)]
17. Ren, P.G.; Liu, X.H.; Ren, F.; Zhong, G.J.; Ji, X.; Xu, L. Biodegradable graphene oxide nanosheets/poly-(butylene adipate-co-terephthalate) nanocomposite film with enhanced gas and water vapor barrier properties. *Polym. Test.* **2017**, *58*, 173–180. [[CrossRef](#)]
18. Raja, V.; Natesan, R.; Thiyagu, T. Preparation and mechanical properties of poly (butylene adipate-co-terephthalate) polyvinyl alcohol/SiO₂ nanocomposite films for packaging applications. *J. Polym. Mater.* **2015**, *32*, 93.

19. Shankar, S.; Rhim, J.-W. Tocopherol-mediated synthesis of silver nanoparticles and preparation of antimicrobial PBAT/silver nanoparticles composite films. *LWT-Food Sci. Technol.* **2016**, *72*, 149–156. [[CrossRef](#)]
20. Shankar, S.; Rhim, J.-W. Preparation of antibacterial poly(lactide)/poly(butylene adipate-co-terephthalate) composite films incorporated with grapefruit seed extract. *Int. J. Biol. Macromol.* **2018**, *120*, 846–852. [[CrossRef](#)]
21. De Campos, S.S.; de Oliveira, A.; Moreira, T.F.M.; da Silva, T.B.V.; da Silva, M.V.; Pinto, J.A.; Bilck, A.P.; Gonçalves, O.H.; Fernandes, I.P.; Barreiro, M.F.; et al. TPCS/PBAT blown extruded films added with curcumin as a technological approach for active packaging materials. *Food Packag. Shelf Life* **2019**, *22*, 100424. [[CrossRef](#)]
22. Xing, Q.; Buono, P.; Ruch, D.; Dubois, P.; Wu, L.; Wang, W.J. Biodegradable UV-blocking films through core-shell lignin-melanin nanoparticles in poly(butylene adipate-co-terephthalate). *ACS Sustain. Chem. Eng.* **2019**, *7*, 4147–4157. [[CrossRef](#)]
23. Sharma, S.; Jaiswal, A.K.; Duffy, B.; Jaiswal, S. Ferulic acid incorporated active films based on poly(lactide)/poly(butylene adipate-co-terephthalate) blend for food packaging. *Food Packag. Shelf Life* **2020**, *24*, 100491. [[CrossRef](#)]
24. Bang, Y.; Shankar, S.; Rhim, J. Preparation of polypropylene/poly(butylene adipate-co-terephthalate) composite films incorporated with melanin for prevention of greening of potatoes. *Packag. Technol. Sci.* **2020**, *33*, 433–441. [[CrossRef](#)]
25. Fereydouni, N.; Darroudi, M.; Movaffagh, J.; Shahroodi, A.; Butler, A.E.; Ganjali, S.; Sahebkar, A. Curcumin nanofibers for the purpose of wound healing. *J. Cell. Physiol.* **2018**, *234*, 5537–5554. [[CrossRef](#)] [[PubMed](#)]
26. Sharma, R.A.; Gescher, A.J.; Steward, W.P. Curcumin: The story so far. *Eur. J. Cancer* **2005**, *41*, 1955–1968. [[CrossRef](#)] [[PubMed](#)]
27. Roy, S.; Rhim, J.-W. Preparation of carbohydrate-based functional composite films incorporated with curcumin. *Food Hydrocoll.* **2020**, *98*, 105302. [[CrossRef](#)]
28. Parvathy, K.S.; Negi, P.S.; Srinivas, P. Antioxidant, antimutagenic and antibacterial activities of curcumin- β -diglucoside. *Food Chem.* **2009**, *115*, 265–271. [[CrossRef](#)]
29. Jagannathan, R.; Abraham, P.M.; Poddar, P. Temperature-dependent spectroscopic evidences of curcumin in aqueous medium: A mechanistic study of Its solubility and stability. *J. Phys. Chem. B* **2012**, *116*, 14533–14540. [[CrossRef](#)] [[PubMed](#)]
30. Chen, Y.; Lin, J.; Fei, Y.; Wang, H.; Gao, W. Preparation and characterization of electrospinning PLA/curcumin composite membranes. *Fibers Polym.* **2010**, *11*, 1128–1131. [[CrossRef](#)]
31. Zia, J.; Paul, U.C.; Heredia-Guerrero, J.A.; Athanassiou, A.; Fragouli, D. Low-density polyethylene/curcumin melt extruded composites with enhanced water vapor barrier and antioxidant properties for active food packaging. *Polymer (Guildf.)* **2019**, *175*, 137–145. [[CrossRef](#)]
32. Musso, Y.S.; Salgado, P.R.; Mauri, A.N. Smart edible films based on gelatin and curcumin. *Food Hydrocoll.* **2017**, *66*, 8–15. [[CrossRef](#)]
33. Roy, S.; Rhim, J.-W. Preparation of antimicrobial and antioxidant gelatin/curcumin composite films for active food packaging application. *Colloids Surf. B Biointerfaces* **2020**, *188*, 110761. [[CrossRef](#)] [[PubMed](#)]
34. Roy, S.; Rhim, J.-W. Carboxymethyl cellulose-based antioxidant and antimicrobial active packaging film incorporated with curcumin and zinc oxide. *Int. J. Biol. Macromol.* **2020**, *148*, 666–676. [[CrossRef](#)] [[PubMed](#)]
35. Ezati, P.; Rhim, J.-W. pH-responsive pectin-based multifunctional films incorporated with curcumin and sulfur nanoparticles. *Carbohydr. Polym.* **2019**, *230*, 115638. [[CrossRef](#)] [[PubMed](#)]
36. Liu, J.; Wang, H.; Wang, P.; Guo, M.; Jiang, S.; Li, X.; Jiang, S. Films based on κ -carrageenan incorporated with curcumin for freshness monitoring. *Food Hydrocoll.* **2018**, *83*, 134–142. [[CrossRef](#)]
37. Aydogdu, A.; Radke, C.J.; Bezci, S.; Kirtil, E. Characterization of curcumin incorporated guar gum/orange oil antimicrobial emulsion films. *Int. J. Biol. Macromol.* **2020**, *148*, 110–120. [[CrossRef](#)] [[PubMed](#)]
38. Chen, H.Z.; Zhang, M.; Bhandari, B.; Yang, C.H. Novel pH-sensitive films containing curcumin and anthocyanins to monitor fish freshness. *Food Hydrocoll.* **2020**, *100*, 105438. [[CrossRef](#)]
39. Varshosaz, J.; Jajanian-Najafabadi, A.; Soleymani, A.; Khajavinia, A. Poly (butylene adipate-co-terephthalate) electrospun nanofibers loaded with 5-fluorouracil and curcumin in treatment of colorectal cancer cells. *Polym. Test.* **2018**, *65*, 217–230. [[CrossRef](#)]
40. Roy, S.; Rhim, J.-W.; Jaiswal, L. Bioactive agar-based functional composite film incorporated with copper sulfide nanoparticles. *Food Hydrocoll.* **2019**, *93*, 156–166. [[CrossRef](#)]

41. Sousa, J.C.; Arruda, S.A.; Lima, J.C.; Wellen, R.M.R.; Canedo, E.L.; De Almeida, Y.M.B. Crystallization kinetics of poly (butylene adipate terephthalate) in biocomposite with coconut fiber. *Rev. Mater.* **2019**, *24*. [[CrossRef](#)]
42. Gennadios, A.; Weller, C.L.; Gooding, C.H. Measurement errors in water vapor permeability of highly permeable, hydrophilic edible films. *J. Food Eng.* **1994**, *21*, 395–409. [[CrossRef](#)]
43. Roy, S.; Rhim, J.-W. Effect of CuS reinforcement on the mechanical, water vapor barrier, UV-light barrier, and antibacterial properties of alginate-based composite films. *Int. J. Biol. Macromol.* **2020**, *164*, 37–44. [[CrossRef](#)] [[PubMed](#)]
44. Roy, S.; Kim, H.C.; Kim, J.W.; Zhai, L.; Zhu, Q.Y.; Kim, J. Incorporation of melanin nanoparticles improves UV-shielding, mechanical and antioxidant properties of cellulose nanofiber based nanocomposite films. *Mater. Today Commun.* **2020**, *24*, 100984. [[CrossRef](#)]
45. Luo, N.; Varaprasad, K.; Reddy, G.V.S.; Rajulu, A.V.; Zhang, J. Preparation and characterization of cellulose/curcumin composite films. *RSC Adv.* **2012**, *2*, 8483–8488. [[CrossRef](#)]
46. Ranjeth Kumar Reddy, T.; Kim, H.J. Mechanical, optical, thermal, and barrier properties of poly(lactic acid)/curcumin composite films prepared using twin-screw extruder. *Food Biophys.* **2019**, *14*, 22–29. [[CrossRef](#)]
47. Shah, S.A.A.; Imran, M.; Lian, Q.; Shehzad, F.K.; Athir, N.; Zhang, J.; Cheng, J. Curcumin incorporated polyurethane urea elastomers with tunable thermo-mechanical properties. *React. Funct. Polym.* **2018**, *128*, 97–103. [[CrossRef](#)]
48. Pramanik, N.; Mitra, T.; Khamrai, M.; Bhattacharyya, A.; Mukhopadhyay, P.; Gnanamani, A.; Kumar Basu, R.; Paban Kundu, P. Characterization and evaluation of curcumin loaded guar gum/polyhydroxyalkanoates blend films for wound healing applications. *RSC Adv.* **2015**, *5*, 63489–63501. [[CrossRef](#)]
49. Wang, L.-F.; Rhim, J.-W. Grapefruit seed extract incorporated antimicrobial LDPE and PLA films: Effect of type of polymer matrix. *LWT* **2016**, *74*, 338–345. [[CrossRef](#)]
50. Moghadamtousi, S.Z.; Kadir, H.A.; Hassandarvish, P.; Tajik, H.; Abubakar, S.; Zandi, K. A review on antibacterial, antiviral, and antifungal activity of curcumin. *Biomed. Res. Int.* **2014**, *2014*, 186864. [[CrossRef](#)]
51. Kaur, S.; Modi, N.H.; Panda, D.; Roy, N. Probing the binding site of curcumin in *Escherichia coli* and *Bacillus subtilis* FtsZ—a structural insight to unveil antibacterial activity of curcumin. *Eur. J. Med. Chem.* **2010**, *45*, 4209–4214. [[CrossRef](#)]
52. Rai, D.; Singh, J.K.; Roy, N.; Panda, D. Curcumin inhibits FtsZ assembly: An attractive mechanism for its antibacterial activity. *Biochem. J.* **2008**, *410*, 147–155. [[CrossRef](#)]
53. Teow, S.-Y.; Liew, K.; Ali, S.A.; Khoo, A.S.-B.; Peh, S.-C. Antibacterial action of curcumin against *Staphylococcus aureus*: A brief review. *J. Trop. Med.* **2016**, *2016*, 1–10. [[CrossRef](#)] [[PubMed](#)]
54. Ak, T.; Gülçin, İ. Antioxidant and radical scavenging properties of curcumin. *Chem. Biol. Interact.* **2008**, *174*, 27–37. [[CrossRef](#)] [[PubMed](#)]

